



FREE VIBRATION AND BUCKLING ANALYSIS ON SMART STRUCTURES

K. SAI SATYANARAYANA, M. DHANVI SANKAR, M. NARESH, G. SWAMY, L. SUDHEER, M. RAMA KRISHNA UG Students, Dept of Mechanical Engineering, GMR Institute of Technology, Rajam.

CH. PRASHANT KUMAR Assistant Professor, Dept of Mechanical Engineering, GMR Institute of Technology, Rajam.

ABSTRACT:

Thin-walled plate and shell structures are one of the most important structural components which are extensively found in civil, aviation and aerospace industries due to their light weight as well as high load-bearing capacity. The advantages of using composite materials are the ability to tailor them for any specific the structural usage, i.e., the material can be optimized by suitably selecting fibre orientation angle and layer thickness.

In this paper, the free vibration and buckling behaviour of laminated structures has been studied. For the buckling and free vibration analysis of the structures, commercial finite element analysis (FEA) software called ABAQUS was employed.

Keywords:

Finite element method, orthotropic plates, Free vibration and buckling analysis

I. Introduction:

Over the past ten years, smart materials and buildings have received a lot of attention. Composite structures with bonded or implanted piezoelectric layers for active vibration control are among the key smart structural systems that have drawn attention. There are very few design tools that are based on an integrated approach that takes into account the sensing, actuation, and control capabilities of smart structures, despite the fact that many finite element-based studies on the design/analysis of structural systems have been conducted in recent years.[1] Composites are a desirable alternative to metallic materials for many structural applications, but their analysis and design are more difficult than those of metallic structures. Through the careful selection of the layer's orientation, number of plies, and stacking order during the fabrication of composite laminates.[2]In the industrial, medical, military, and scientific fields, smart structures are frequently created using piezoelectric materials. Many engineers and researchers have developed more precise and effective analytical methods for forecasting behaviours of piezoelectric laminated plates in recent years due to the expanding application of piezoelectric effects in smart and intelligent structures.[3]

For analysing the vibrational behaviour of composite structures, several computational methods, such as analytical techniques, the differential quadrature method, the finite element method (FEM), and the Rayleigh-Ritz approach, have recently been developed. Also, a number of experimental experiments have been carried out to determine the vibrational properties of composite structures.[4]In hybrid composites, several fibres of various kinds are incorporated into a single matrix. The mechanical properties of these materials are a weighted average of their constituent parts, with a more desirable balance between their benefits and drawbacks.Using smart hybrid composite structures in engineering applications is also being encouraged by the introduction of novel smart structures that have distributed sensors and actuators for controlling certain mechanical behaviours. The most frequent components added to composite structures to improve their qualities for various uses are SMA wires and piezoelectric actuators. Smart composite structures and papers pertaining to their optimisation are included in this subsection. In order to achieve the highest buckling load, Correia et al. tuned the position of the piezoelectric actuators and the fibre orientation angles incorporated into the piezoelectric laminated composite plates.[5]



II. Functionally graded piezoelectric material (FGPM) plate :

Consider a rectangular FGPM plate that has layers of piezoelectric material on the top and bottom which is shown in Fig 1. We postulate that the substrate's characteristics always vary along its thickness, resulting in top and bottom surfaces that are respectively rich in PZT-4 and PZT-5H.

Here, we use the cartesian coordinates $x; y; z$, where x & y are the in-plane axes of neutral surfaces, and z is the standard axis. The FGPM Plate's effective qualities, which change depending on the direction of thickness and are made of two types of piezoelectric material, are as follows: [1]

$$P_{eff}(z) = P_u V_u(Z) + P_1(1-V_u(z)) \dots \dots \dots [1]$$

P_u & P_1 are the higher and lower surface properties of the FG piezoelectric material plate, V_u is the volume fraction, n is power-law exponent, and P_{eff} is the effective material properties, the equation is expressed as follows:

$$V_u = \left(\frac{z}{h} + 0.5\right)^n \dots \dots \dots [2]$$

$$P(z) = P_{ul} + \left(0.5 + \left(\frac{z}{h}\right)^n + P_l \dots \dots \dots [3]$$

III. Finite Element Formulation:

The FSDT established the displacement field of a random point in the rectangular FGPM plate as :

$$u(x,y,z,t) = u_0(x,y,t) + z\beta_1(x,y,t) \dots \dots \dots [4a]$$

$$v(x,y,z,t) = v_0(x,y,t) + z\beta_2(x,y,t) \dots \dots \dots [4b]$$

$$w(x,y,z,t) = w_0(x,y,t) \dots \dots \dots [4b]$$

$u, v,$ and w are variables that denote displacements along the corresponding $x, y,$ and z axes. The numbers β_1 & β_2 stand in for the bending rotation, and the letters u_0, v_0 & w_0 denote impartial surface displacements. According to the displacement field in Eq. (4), the strain is as follows:

$$\epsilon_{11} = (\partial u_0 / \partial x) + z (\partial \beta_1 / \partial x) \dots \dots \dots [5a]$$

$$\epsilon_{22} = (\partial v_0 / \partial y) + z (\partial \beta_2 / \partial y) \dots \dots \dots [5b]$$

$$\epsilon_{12} = (\partial u_0 / \partial y) + (\partial v_0 / \partial x) + z [(\partial \beta_1 / \partial y) + (\partial \beta_2 / \partial x)] \dots \dots [5c]$$

$$\epsilon_{13} = (\partial W / \partial x) + \beta_1, \epsilon_{23} = (\partial W / \partial y) + \beta_2 \dots \dots \dots [5d]$$

The electrical and mechanical interactions of piezo-electric materials are defined by the linear constituent relationships.

$$\sigma = [Q] \{ \epsilon \} - [e] \{ E \} \dots \dots \dots [6]$$

$$\{ D \} = [e]^T \{ \epsilon \} + [\epsilon] \{ E \} \dots \dots \dots [7]$$

$$\{ \tau \} = [E_s] \{ \epsilon_s \} \dots \dots \dots [8]$$

Here, $[Q], [e], [\epsilon]$ and $[E_s]$ are elastic constant matrices, as well as piezoelectric, dielectric, and elastic shear constants. The total potential energy U for the FGPM plate can be represented as follows:



$$U = \frac{1}{2} \left[\int_v \{\varepsilon\}^T \{\sigma\} \right] dV + \frac{1}{2} \left[\int_v \{\varepsilon_s\}^T \{\tau\} - \int_v \{E\} \{D\} \right] dV \dots [9]$$

The displacement and electric potential of the nodal component are as follows:

$$\{u\} = [H][N_u]\{u^e\} \dots \dots \dots [10]$$

$$\{\phi\} = [N_\phi] \{\phi^e\} \dots \dots \dots [11]$$

$$\psi_i = \frac{1}{4} (1 + \zeta_i \zeta) (1 + \varsigma_i \varsigma) \dots \dots \dots [12]$$

i = 1,2,3,4

Where $[N_u]$ and $[N_\phi]$ are the shape function matrices, $\{u^e\}$ and $\{\phi^e\}$ are the global nodal displacements and the global nodal electric potentials, respectively, and is ψ_i linear interpolation functions, $\varsigma = y/b$, $\zeta = x/a$. The following are the formulas for the tiny engineering strains related to displacement:

$$\{\varepsilon\} = ([B_u]\{u^e\}) \dots \dots \dots [13]$$

The electric field (E_f) related vector is represented by nodal variables as:

$$\{E_f\} = - \Delta \phi = -(\{\phi^e\}[B_\phi]) \dots \dots \dots [14]$$

Equation (15) for the modal analysis of functionally graded piezoelectric material plate is obtained by solving Equations (6), (13), (14), and (9) as follows:

$$|([K_u] - \omega^2[M_u])| = 0 \dots \dots \dots [15]$$

IV. Results and Discussion:

This section uses finite element analysis simulation to examine the static and modal analysis responses of the rectangular FG piezoelectric material plate while applying various boundary conditions. Three processes make up the simulation process in the ANSYS package: pre-treatment, solution, and postprocessing. To validate the stability and viability of the finite element models based on the aforementioned theory, the results of the present model are compared with the existing methodology described in the literature. The FGPM rectangular plate is made of PZT-4 and PZT-5H, and the material characteristics are ranked in the thickness direction described by Eqs. (2) and (3). (3). The FGPM plate has PZT-4 and PZT-5H-rich surfaces on the top and bottom, respectively.

4.1 Results for composite plate:

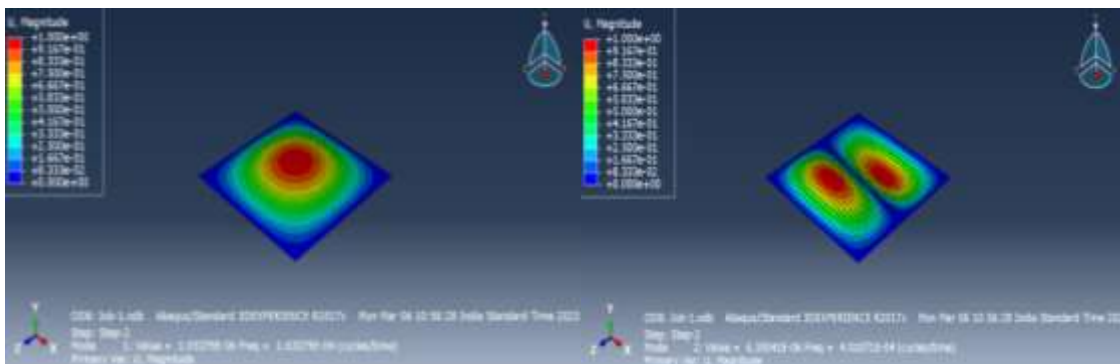
The first four mode shapes are obtained, and the frequency and corresponding displacement values are determined. The buckling behaviour of the plate is also determined. The mode shapes show the bending behaviour of the plate in different directions. The results are compared with the analytical solutions, and a good agreement is observed.

4.2 Material Properties for Piezoelectric Patch:

ELASTIC MODULE, E (N/mm ²)	PIEZOELECTRIC MATERIAL
Density	7500
Dielectric (Electrical Permittivity)	
D11	5.87E-009
D12,D13 ,D23	0
D22 , D33	6.75E-009
Elastic	
D1111	115000000000
D1122, D1133	74300000000
D2222	139000000000
D2233	77800000000
D3333	139000000000
D1212, D1313,D2323	25600000000
Piezoelectric	
e1 11	15.08
e1 22,e1 33	-5.207
e1 12, e1 13, e1 23, e2 11, e2 22, e2 33, e2 13, e2 23, e3 11, e3 22 e3 12, e3 23	0
e2 12, e3 13	12.71

4.3 Material Properties for Composite Material (Graphite/Epoxy):

ELASTIC MODULE, E (N/mm ²)	GRAPHITE / EPOXY
Density	1446.2
Elastic	
Type Lamina	
E1 (Gpa)	132000 N/Sq mm
E2 (Gpa)	5350 N/Sq mm
Nu12	0.3
G12 (Gpa)	2790 N/Sq mm
G13 (Gpa)	2790 N/Sq mm
G23 (Gpa)	1395 N/Sq mm



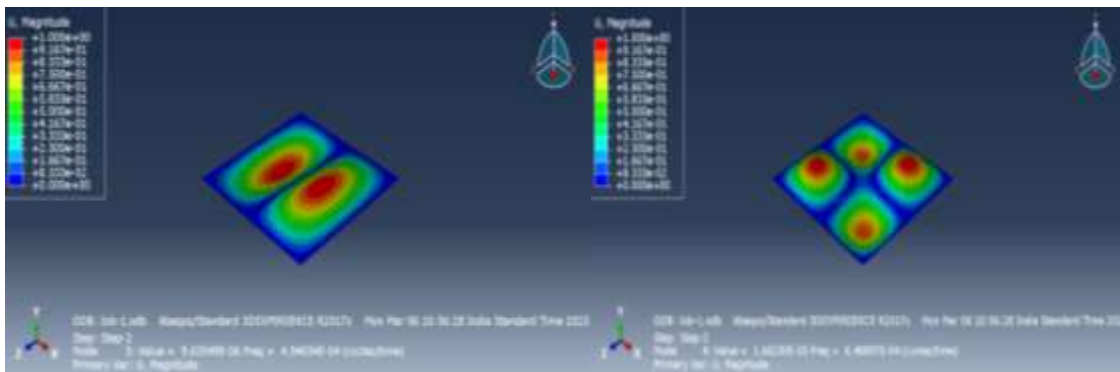


Figure 1: Deformations of square plate with different frequencies under SSSS boundary condition

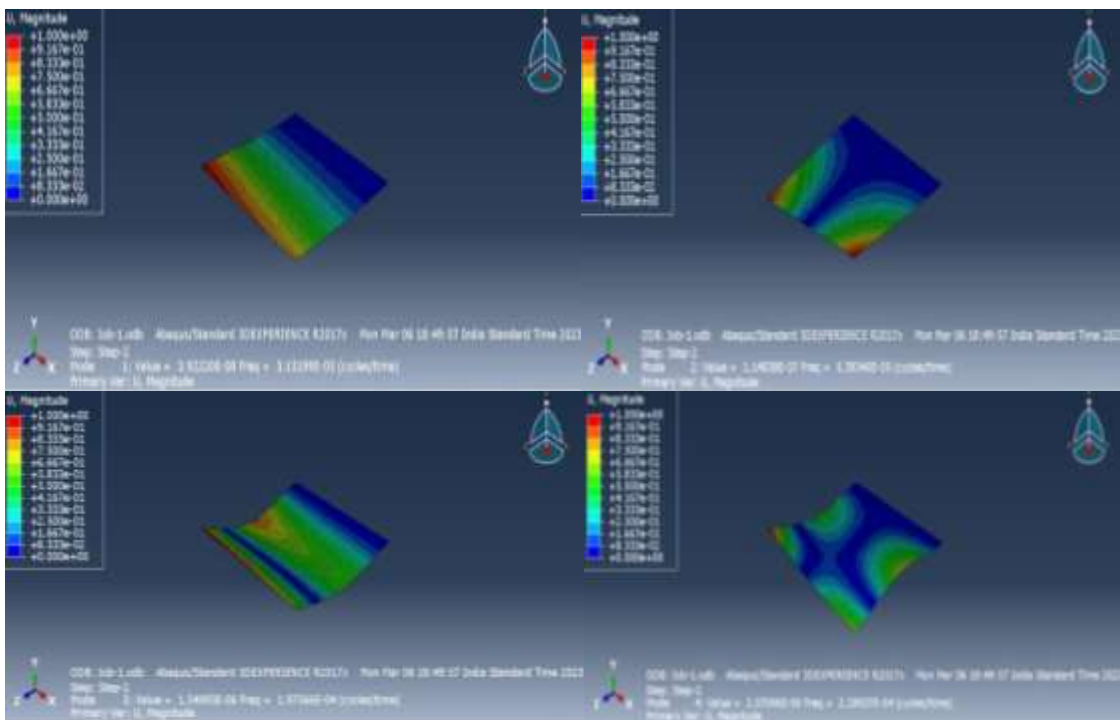
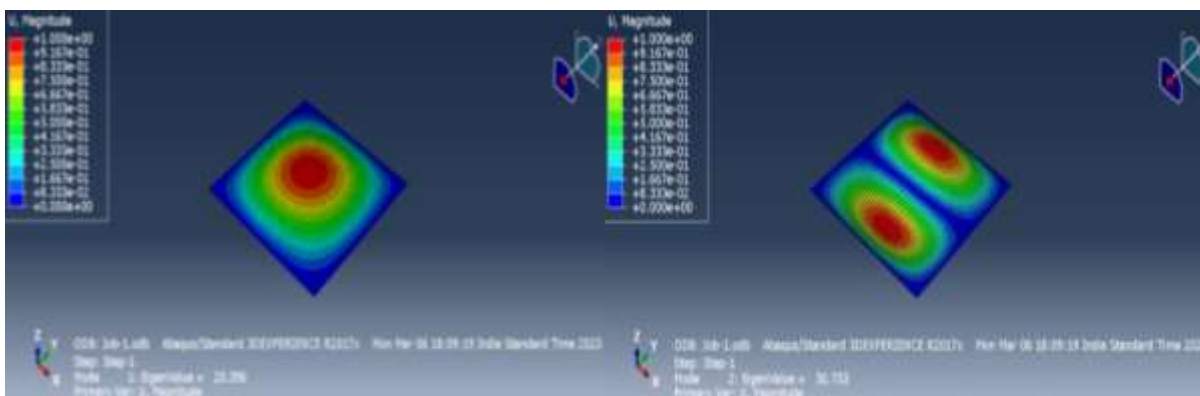


Figure 2: Deformations of square plate with different frequencies under CFFF boundary condition



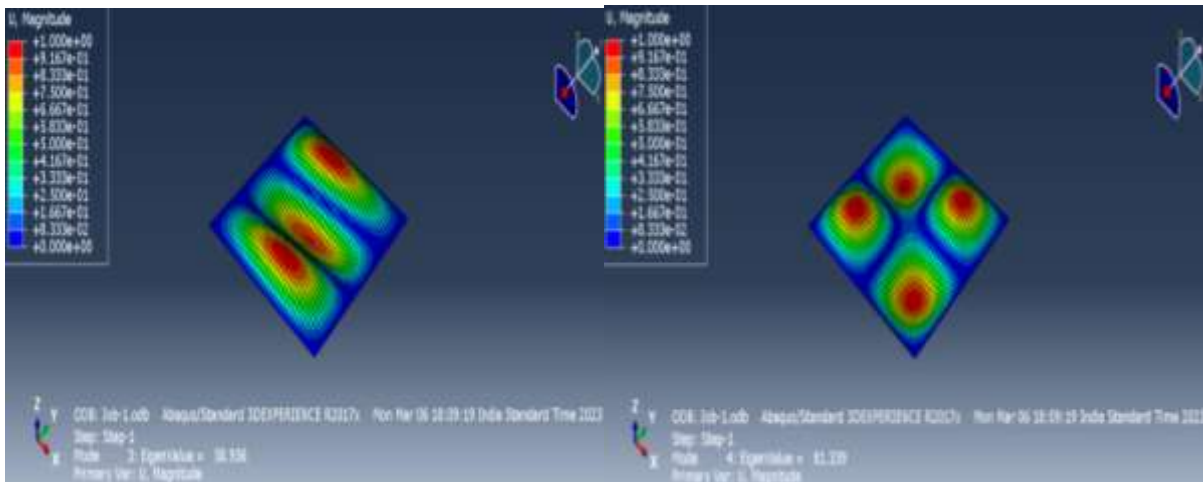


Figure 3: Deformations of square plate with different Eigen values under SSSS boundary condition

Table 1: Comparison of natural frequency of composite plate

Boundary condition		Mode 1	Mode 2	Mode 3	Mode 4
SSSS	Present	163.37	401.07	494.03	648.89
	[6]	163.37	400.48	493.18	648.91
	[7]	164.37	404.38	492.29	658.4
CFFF	Present	31.51	53.93	197.56	229.03
	[6]	41.14	60.50	220.39	257.28
	[7]	41.34	60.66	221.52	258.72

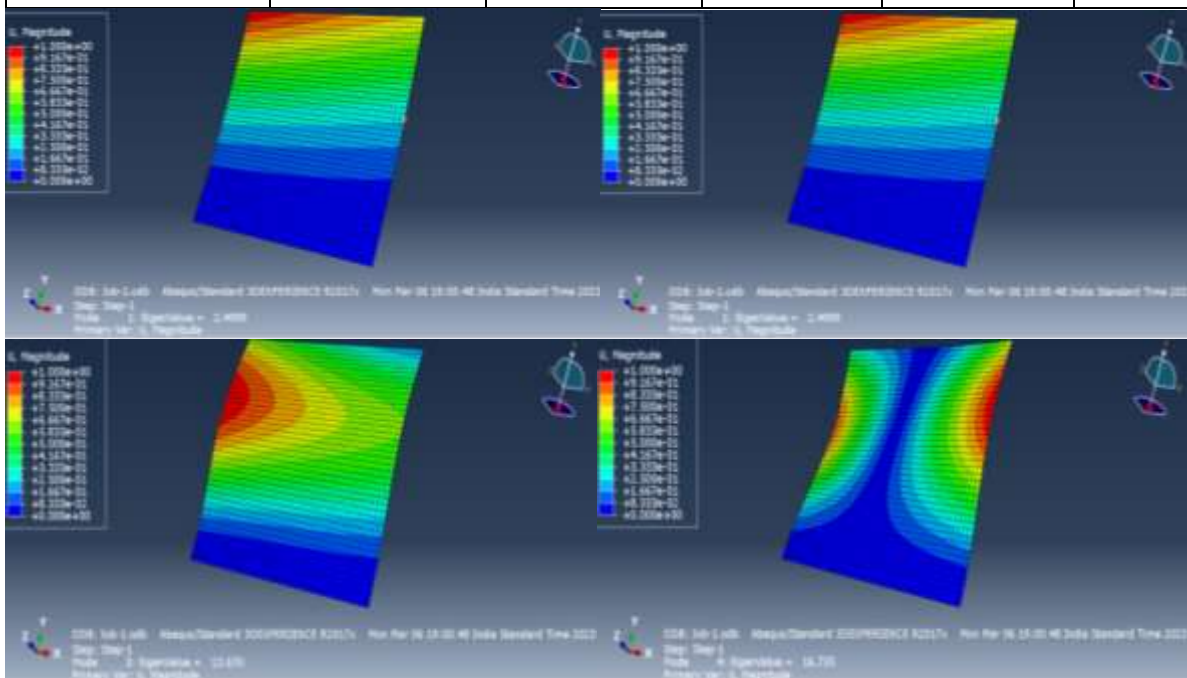


Figure 4: Deformations of square plate with different Eigen values under CFFF boundary condition



Table 2: Difference between Theoretical and Experimental Results

S. No.	Weights	Voltage(volts)	Current(Amps)	Power(Watts)Experimental
1.	16-20	1.6	0.015	0.024
2.	21-25	2.1	0.032	0.067
3.	26-30	2.4	0.054	0.129
4.	31-35	2.8	0.073	0.204
5.	36-40	3.4	0.098	0.332

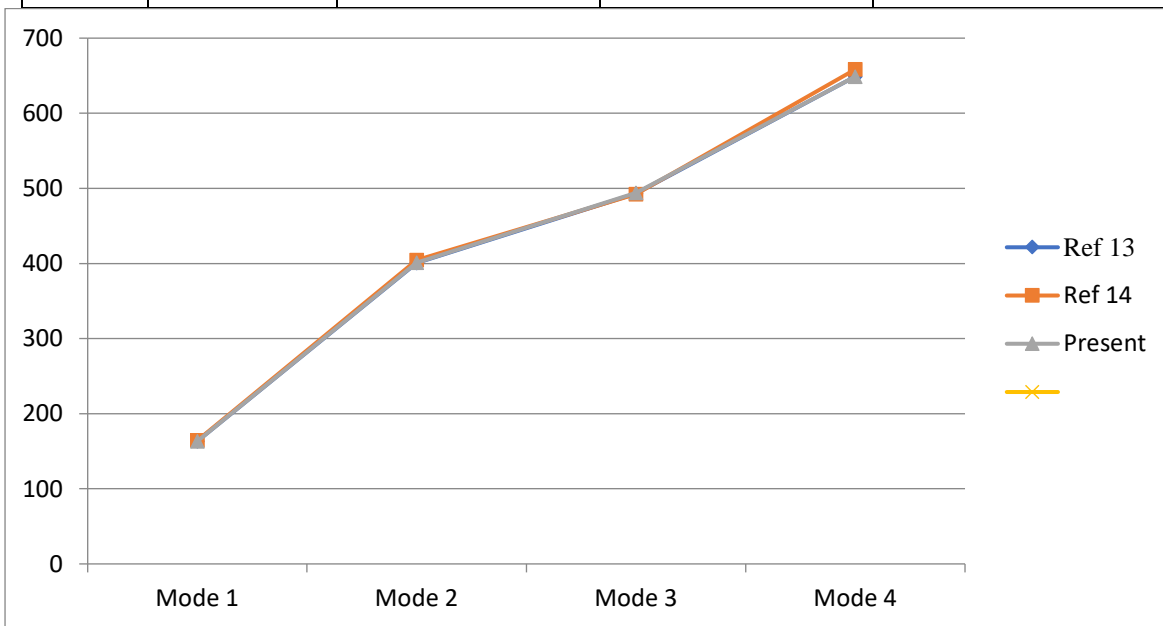


Figure 5: Graphical representation of Natural frequency results under SSSS boundary condition.

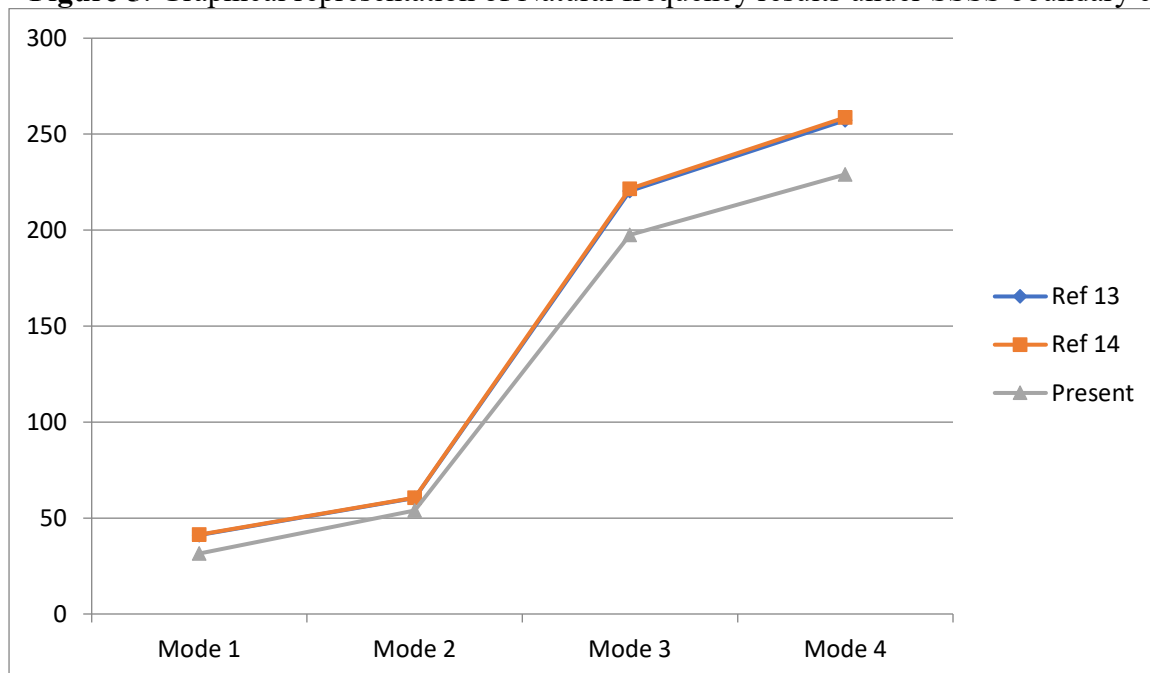


Figure 6: Graphical representation of Natural frequency results under CFFF boundary condition



V. Conclusion:

In this paper symmetrically layered square composite plate has analyzed with the help of ABAQUS software which uses finite element analysis methods. The natural frequencies of the composite plates were determined using the finite element approach for different plate edge conditions as well as random plate length/width ratios and layer number. Through the integration of sensors, smart composite structures can achieve optimal performance and enhanced functionality. However, the design and analysis of these structures pose significant challenges, including material selection, geometric complexity, and computational limitations. As a result, there is a need for continued research and development in this field to address these challenges and further improve the performance of smart composite structures.

- The natural frequencies of the plates are greater under the S-S-S-S boundary condition than under the C-F-F-F boundary condition.
- As a result, the frequencies of the plates are significantly reliant on their boundary conditions.
- The maximum fundamental natural frequency of a thick plate is demonstrated to be affected by boundary conditions, the number of layers, and the thickness-to-length ratio.
- The obtained results have been compared with the previously verified results of researchers and shown.

VI. Reference:

- 1) Koko, T.S., Orisamolu, I.R., Smith, M.J. and Akpan, U.O., 1997, June. Finite-element-based design tool for smart composite structures. In *Smart Structures and Materials 1997: Mathematics and Control in Smart Structures* (Vol. 3039, pp. 125-134). SPIE.(Finite element based design tool for smart composite structures)
- 2) Fathallah, E., Qi, H., Tong, L. and Helal, M., 2015. Design optimization of lay-up and composite material system to achieve minimum buoyancy factor for composite elliptical submersible pressure hull. *Composite Structures*, 121, pp.16-26. (Design optimization of lay-up and composite material system to achieve minimum buoyancy factor for composite elliptical submersible pressure hull)
- 3) Tanzadeh, H. and Amoushahi, H., 2019. Buckling and free vibration analysis of piezoelectric laminated composite plates using various plate deformation theories. *European Journal of Mechanics-A/Solids*, 74, pp.242-256. (Buckling and Free Vibration Analysis of Piezoelectric Laminated Composite Plates using Various Plate Deformation Theories)
- 4) Ansari, E., Hemmatnezhad, M. and Taherkhani, A., 2023. Free vibration analysis of grid-stiffened composite truncated spherical shells. *Thin-Walled Structures*, 182, p.110237.(Free vibration analysis of grid-stiffened composite truncated spherical shells)
- 5) Nikbakt, S., Kamarian, S. and Shakeri, M., 2018. A review on optimization of composite structures Part I: Laminated composites. *Composite Structures*, 195, pp.158-185.(A Review on Optimization of Composite Structures Part I: Laminated Composites)
- 6) F. Ju, H.P. Lee, K.H. Lee, Finite element analysis of free vibration of delaminated composite plates, *Compos. Eng.* 5 (1995) 195–209.
- 7) Ganesh Shankar, S. Keshava Kumar, P.K. Mahato, Vibration analysis and control of smart composite plates with delamination and under hygrothermal environment, *Thin-Walled Structures*, Volume 116, (2017) 0263-8231.